

IAEA-TECDOC-Draft No 3

Handbook on photonuclear data for applications

Cross sections and spectra

Final report of a co-ordinated research project

March 2000

FOREWORD

Nuclear data for applications constitute an integral part of the IAEA's programme of activities. In recent years, the traditional emphasis on energy applications, in terms of nuclear power reactors and related neutron reaction data, has been gradually shifting towards non-energy applications. This shift could be viewed as a response to increasing user demands for data describing nuclear interactions with charged particles and photons.

Photons are commonly produced as bremsstrahlung radiation by electron accelerators. These are relatively simple machines present in many hospitals, industries and laboratories. Photonuclear data, describing interactions of photons with atomic nuclei, are of importance for a variety of applications. These applications span from radiation shielding and radiotherapy to inspection technologies and possibly nuclear waste transmutation.

In response to growing needs for photonuclear data, in the 1990's, a number of laboratories worldwide became engaged in the development of their own or national photonuclear data libraries. There was no international coordination of this effort, and consequently no effort to create an internationally recognized photonuclear data library.

In this situation the IAEA initiated a Coordinated Research Project (CRP) under the title "*Compilation and Evaluation of Photonuclear Data for Applications*". The project, coordinated by the IAEA between 1996 and 1999, produced three major results: the IAEA Photonuclear Data Library; the present Handbook on Photonuclear Data for Applications; and additions of compiled experimental photonuclear cross sections in the EXFOR database.

The IAEA wishes to thank all the participants of the CRP and other scientists for their work that led to the creation of the Photonuclear Data Library and for their contributions to the present TECDOC. The assistance of M.B. Chadwick (chair), A.I. Blokhin, T. Fukahori, Y.-O. Lee, M.N. Martins, V.V. Varlamov, B. Yu, as well as Y. Han, S.F. Mughabghab, and J. Zhang, in the preparation of this publication is gratefully acknowledged. The responsible IAEA staff member for this report was P. Obložinský, Division of Physical and Chemical Sciences.

Contents

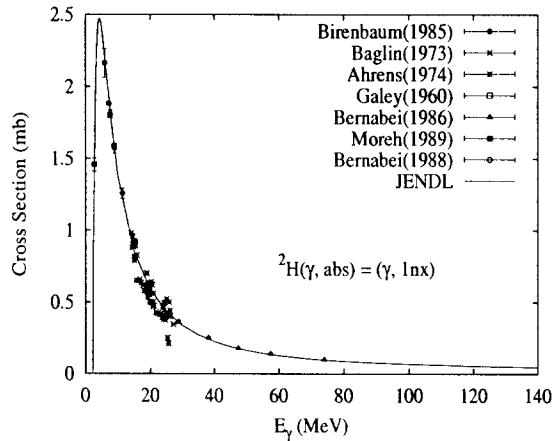
1	Introduction	1
2	Definitions and Notation	5
2.1	General	5
2.2	Symbols	7
2.3	Abbreviations	7
3	Available Experimental Data	8
3.1	Experiments	8
3.1.1	Bremsstrahlung	8
3.1.2	Positron Annihilation in Flight	9
3.1.3	Bremsstrahlung Tagging	11
3.1.4	Electron-induced Reactions	12
3.2	Compiled Data	14
3.2.1	Bibliographic Data	14
3.2.2	EXFOR Library	16
3.2.3	Atlases of Cross Sections and GDR Parameters	16
3.2.4	Additional Data in Other Formats	17
3.3	Access to Data	18
4	Nuclear Models	19
4.1	Photoabsorption Model	19
4.2	Reaction Models	21
4.2.1	Preequilibrium Emission	21
4.2.2	Compound Nucleus Equilibrium Emission	23
4.2.3	Illustrative Comparisons with Experiment	23
4.2.4	Angular Distributions	25
4.2.5	Photofission	27
4.3	Nuclear Modeling Codes	31
4.3.1	GNASH (Los Alamos)	31
4.3.2	ALICE-F and MCPHOTO (Tokai)	31
4.3.3	GUNF and GLUNF (Beijing)	32
4.3.4	XGFISS (Obninsk)	33
4.4	Relation Between Electron and Photon Induced Reactions	33
5	Evaluations	36
5.1	Evaluations Based on Experimental Data	36
5.2	Evaluations Based on Model Calculations	38
5.2.1	Emission Spectra	40
5.3	Methods Used for Producing Evaluated Libraries	41
5.3.1	Obninsk Library (BOFOD)	41
5.3.2	Beijing Library (CNDC)	42
5.3.3	Moscow Library (EPNDL)	43
5.3.4	JENDL Library (JENDL)	43
5.3.5	KAERI Library (KAERI)	44

5.3.6	Los Alamos Library (LANL)	45
6	IAEA Photonuclear Data Library	48
6.1	Selection Procedure	48
6.2	Contents of the Library	55
6.3	ENDF-6 Format	57
6.4	Access to the Library	59
7	Recommendations to Users and Evaluators	61
	References	62
A	Atlas of Giant Dipole Resonances	69
B	IAEA Photonuclear Data library: Graphical Presentation	91
	Contributors to Drafting and Review	273



$$\gamma + {}^2\text{H}$$

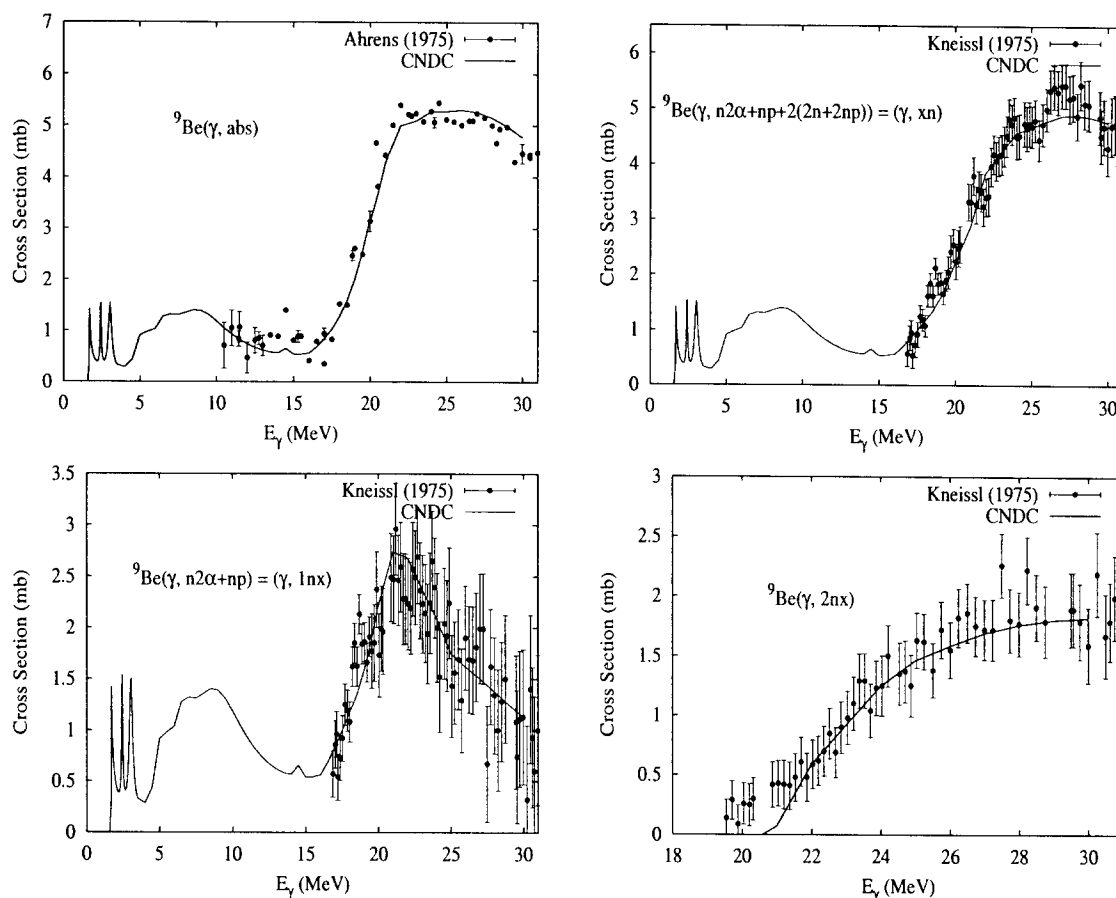
Abundance (%)	Threshold Energies (MeV)								
	γ, n	γ, p	γ, t	$\gamma, \text{He-3}$	γ, α	$\gamma, 2n$	γ, np	$\gamma, 2p$	$\gamma, 3n$
0.01	2.22	*	*	*	*	*	*	*	*



Deuteron's low photoneutron threshold (2.22 MeV) makes it an important potential neutron source in applications that include heavy water. Because of its light mass, the nuclear theories described in this report are unsuitable for modeling deuteron photodisintegration. Instead, use was made of models of Marshall + Guth [Mar50] and Partovi [Par64]. Furthermore, the evaluation was closely based on the measurements of [Ale68, All55, Bar52a, Bar52b, Bir85, Bis50, Deb92, Gal60, Hal53, Hou50, Kec56, McM55, Mor89, Phi50, Sne50, Waf51, Wha56]. Angular distributions of the photoneutrons are provided in the evaluation. Further details are given in [Mur94].

$\gamma + {}^9\text{Be}$

Abundance (%)	Threshold Energies (MeV)							
	$\gamma, n+2\alpha$	γ, p	γ, t	$\gamma, \text{He-3}$	$\gamma, 2n$	γ, np	$\gamma, 2p$	$\gamma, 3n$
100.00	1.67	16.89	17.69	21.18	20.56	18.92	29.34	31.24

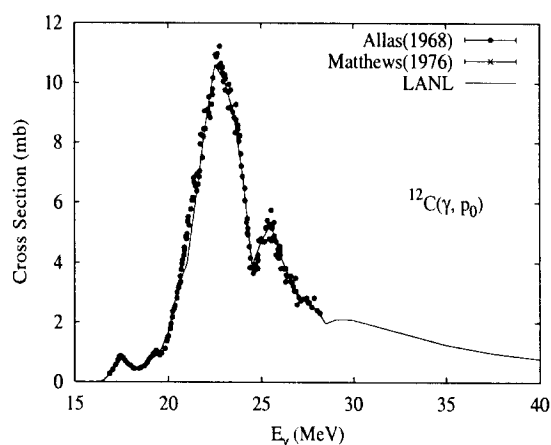
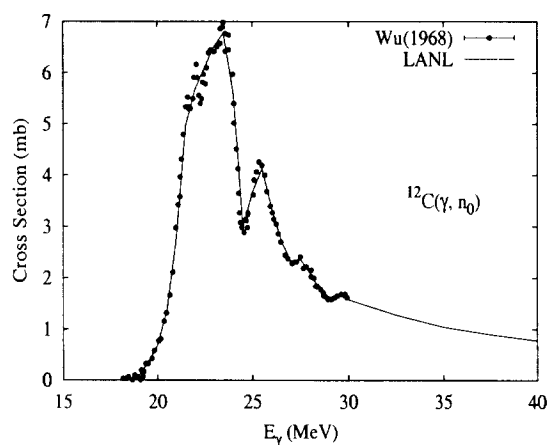
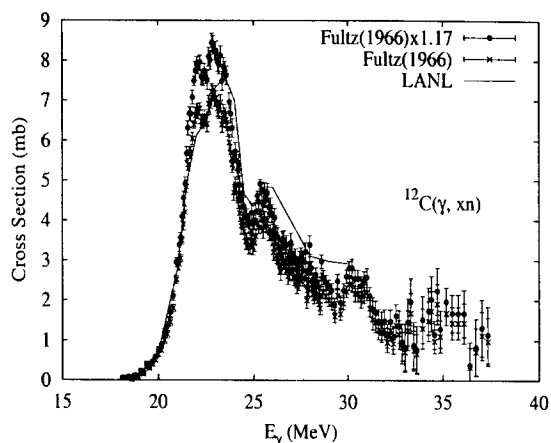
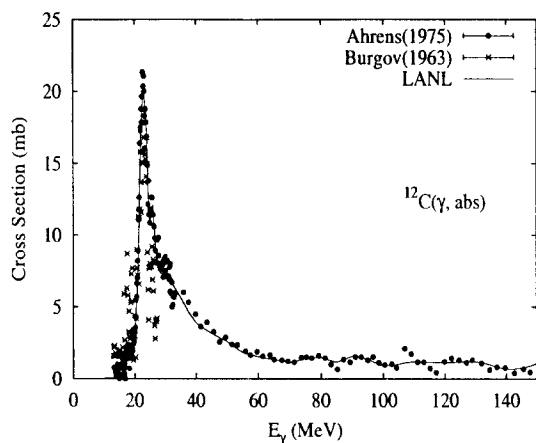


The measured data of $\sigma(\gamma, \text{abs})$ are taken from J.Ahrens [Ahr75] and the photonuclear data of $(\gamma, 1n)$, $(\gamma, 2n)$, (γ, np) reactions are taken from U.kneissl [Kne75], R.D.Edge [Edg57], J.H.Gibbons [Gib59], W.John [Joh62] and M.Fujishiro [Fuj82]. The experimental data were evaluated to guide the model calculation with code GLUNF [Zha99] up to 30 MeV, in which the file 6 in ENDF/B-VI format are given with full energy balance. However, below 16 MeV, the model calculation could not reproduce the experimental data of the $(\gamma, 1n)$ reaction, while these data have been performed by T.Fukohari [Fuk99] by using GDR multiple Lorentzian fitting, which have been adopted in this work.

At low energy (< 30 MeV), the giant-dipole resonance is the dominant excitation mechanism, in this energy region a simple isotropic approximation was used for the angular distribution of outgoing particles. The double differential cross sections include $(\gamma, 1n)$, $(\gamma, 2n)$, (γ, np) reaction channels. In the (γ, np) reaction channel, the spectra of neutron, proton, ${}^7\text{Li}$ and gamma as well as gamma-Multiplicity are involved in the file 6.

$$\gamma + {}^{12}\text{C}$$

Abundance (%)	Threshold Energies (MeV)								
	γ, n	γ, p	γ, t	$\gamma, \text{He-3}$	γ, α	$\gamma, 2n$	γ, np	$\gamma, 2p$	$\gamma, 3n$
98.89	18.72	15.96	27.37	26.28	7.37	31.84	27.41	27.19	53.13



Our evaluation of photonuclear reactions on carbon follows, to a large extent, the analysis described by Fuller [Ful85].

The photoabsorption cross section was evaluated based on the data of Ahrens [Ahr75], that extend up to 150 MeV. Below 30 MeV, a constant value of 0.7 mb was subtracted from these data, as recommended by Fuller.

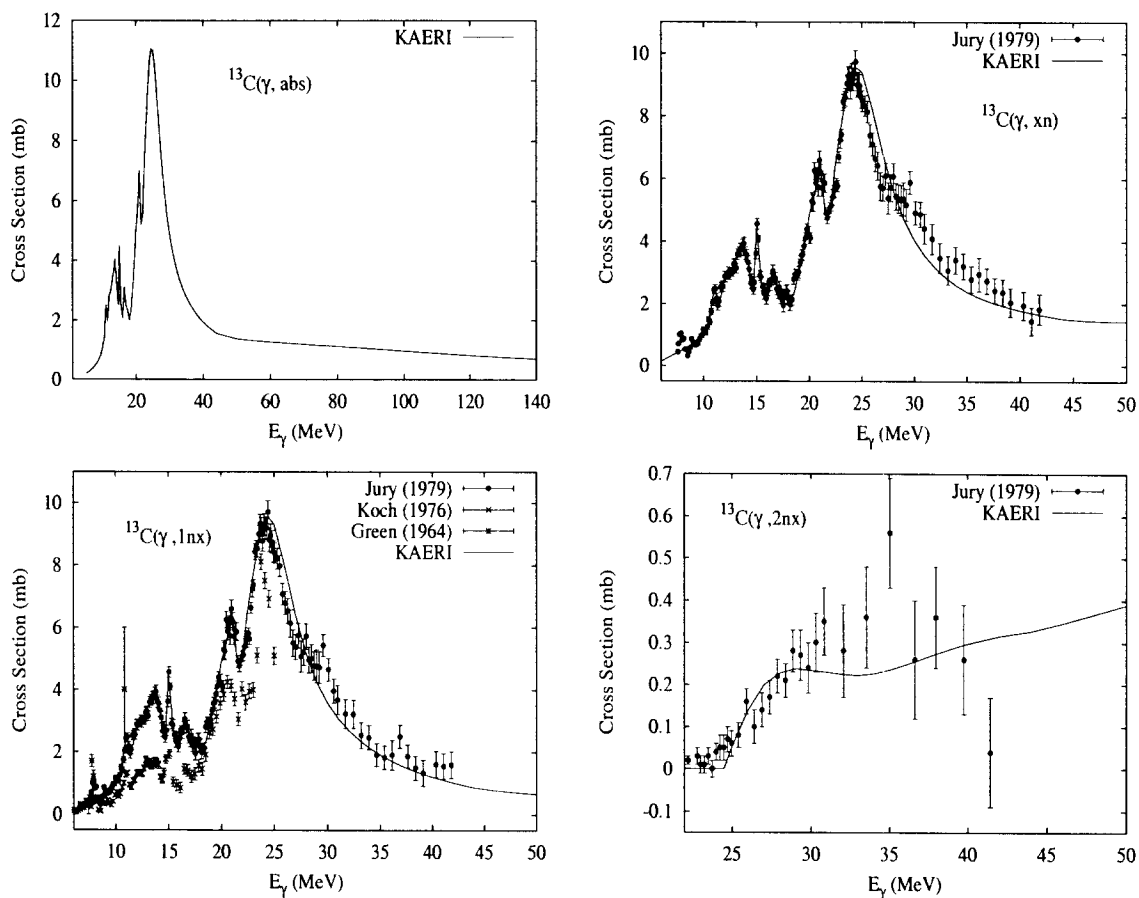
The Hauser-Feshbach statistical theory cannot be immediately applied in the analysis of photonuclear reactions on carbon, since there are significant contributions from direct reactions. In particular the (γ, n_0) and (γ, p_0) processes, which result in the residual nucleus being left in its ground state, account for a significant fraction of the photonuclear cross section (particularly for incident energies below 30 MeV). Therefore we first evaluate the (γ, n_0) and (γ, p_0) cross sections from the available experimental data. We adopt Fuller's recommendations [Ful85] in the GDR region; at higher energies our evaluation is based on the Matthews [Mat76] data at 60, 80, and 100 MeV for (γ, p_0) reactions, and we assume an equal cross section for the (γ, n_0) reactions at these high energies motivated by the concept of QD reaction mechanism. We used dipole angular distribution shapes (the only non-zero Legendre coefficient being a_2) taken from Fuller. This describes the angular distribution in the GDR region. Although it is not appropriate at higher energies, where forward peaking is observed [Cha95a], our present evaluation is probably adequate

for most applications since the (γ, n_0) and (γ, p_0) reactions become very small in magnitude at higher incident energies.

The remaining cross section after (γ, n_0) and (γ, p_0) processes have occurred is modeled with the GNASH code, and represented in the ENDF file using MT5. Preequilibrium and compound decay processes are included. The resulting neutron emission contribution, when added to the (γ, n_0) cross section, was compared with Fuller's evaluation based on a renormalization of Fultz's data [Ful66] by a factor 1.17. Reasonable agreement for neutron production was obtained in the GDR peak, though the calculations appeared to somewhat overpredict neutron production (by as much as 30%) by 30 MeV. This failing is due to the difficulties in using a Hauser-Feshbach code to model reactions on light nuclei. Finally, GNASH calculations [Cha95a] of proton emission spectra for 60 MeV incident photons agreed well with the DDX data of McGeorge [McG86].

$\gamma + {}^{13}\text{C}$

Abundance (%)	Threshold Energies (MeV)								
	γ, n	γ, p	γ, t	$\gamma, \text{He-3}$	γ, α	$\gamma, 2n$	γ, np	$\gamma, 2p$	$\gamma, 3n$
1.11	4.95	17.53	23.88	24.41	10.65	23.67	20.90	31.63	36.79

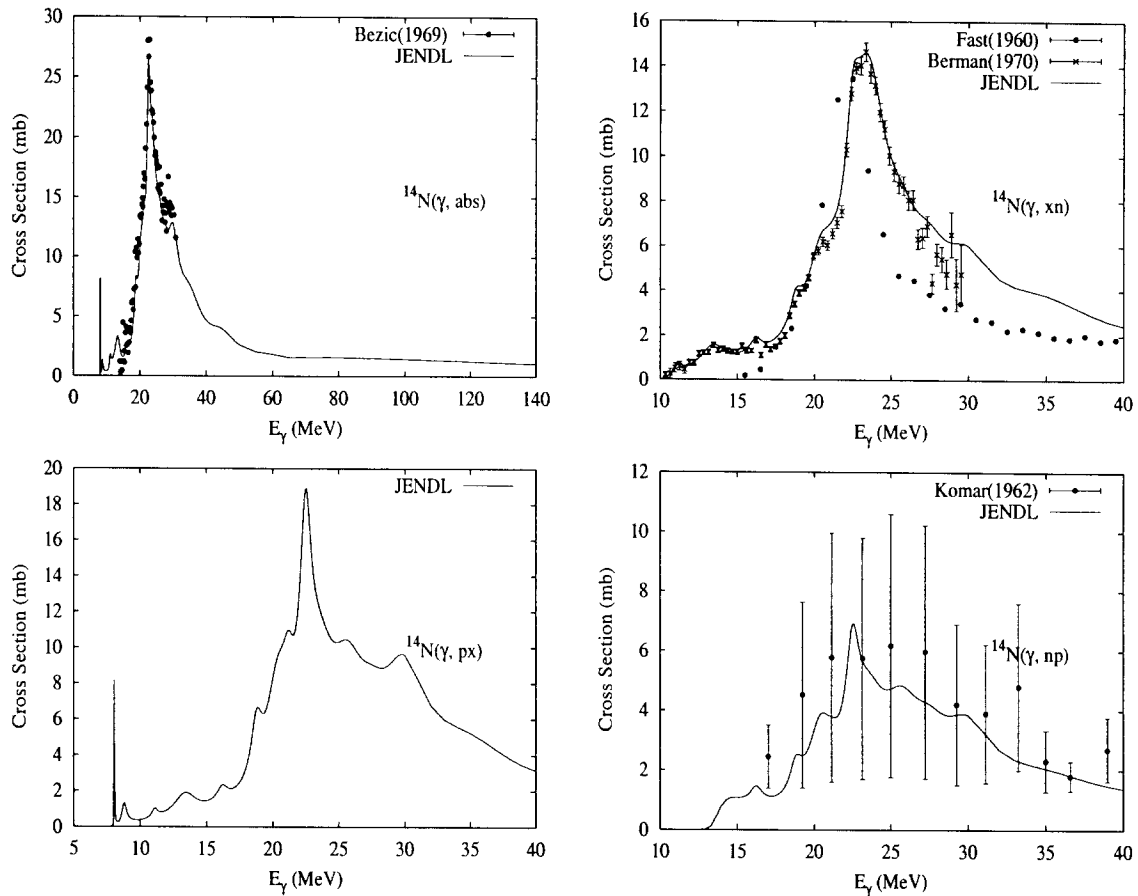


The photoabsorption cross section has not been measured. However, there are experimental data for the $(\gamma, 1nx)$, $(\gamma, 2nx)$ and (γ, xn) reaction cross sections [Jur79, Koc76, Gre64]. We relied on the GUNF and GNASH codes to infer the photoabsorption cross section in the GDR regime, in order to model accurately Jury's $(\gamma, 1nx)$ data. The photoabsorption cross section above the GDR, up to 140 MeV, was obtained from QD model calculations using the theory of Chadwick.

The calculated results of the emission channels by the GNASH code are in good agreement with the Jury data for the $(\gamma, 1nx)$, $(\gamma, 2nx)$ and (γ, xn) cross sections.

$\gamma + {}^{14}\text{N}$

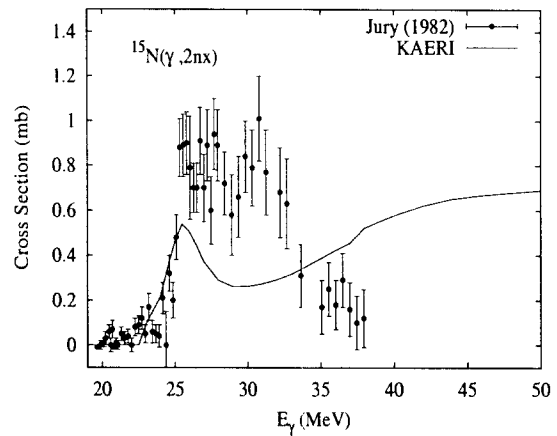
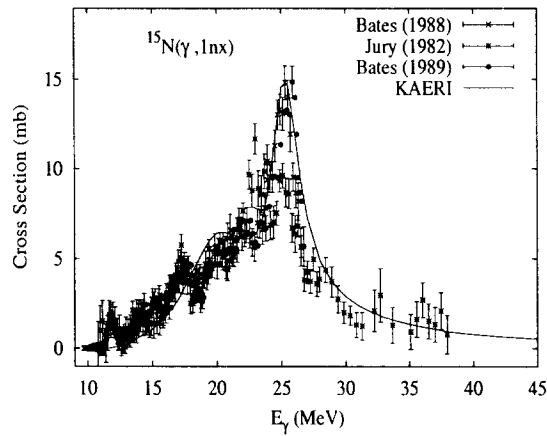
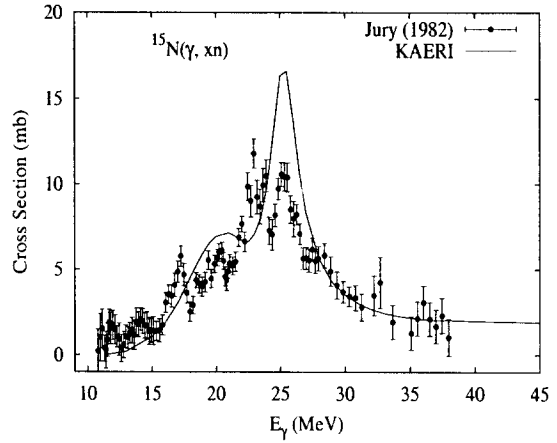
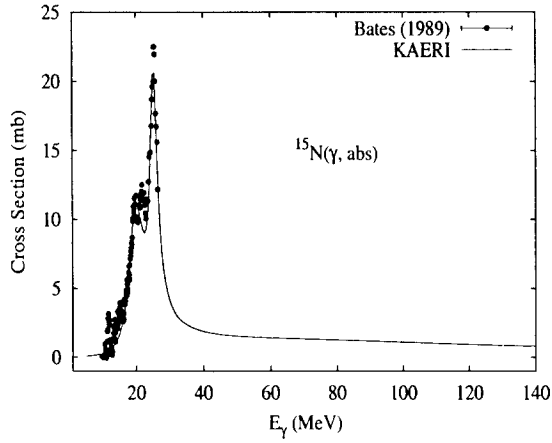
Abundance (%)	Threshold Energies (MeV)								
	γ, n	γ, p	γ, t	$\gamma, \text{He-3}$	γ, α	$\gamma, 2n$	γ, np	$\gamma, 2p$	$\gamma, 3n$
99.63	10.55	7.55	22.74	20.74	11.61	30.62	12.50	25.08	46.24



The photoabsorption cross section was measured by Bezić et al. [Bez69] and was analyzed between 15 and 31 MeV. Above 31 MeV, the cross section was estimated based on measurements of ${}^{16}\text{O}$ and ${}^{12}\text{C}$. Total photoneutron production data below 30 MeV [Ber70] were analyzed consistently together with other reaction channels [Kom62]. Above 30 MeV, the cross section was calculated with a GDR plus QD models [Mur91].

$\gamma + {}^{15}\text{N}$

Abundance (%)	Threshold Energies (MeV)								
	γ, n	γ, p	γ, t	$\gamma, \text{He-3}$	γ, α	$\gamma, 2n$	γ, np	$\gamma, 2p$	$\gamma, 3n$
0.37	10.83	10.21	14.85	28.20	10.99	21.39	18.38	31.04	41.45

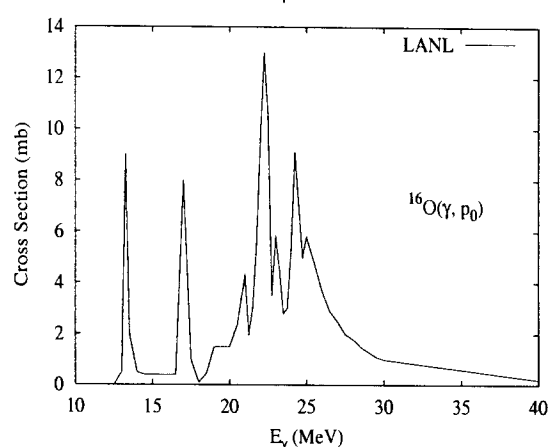
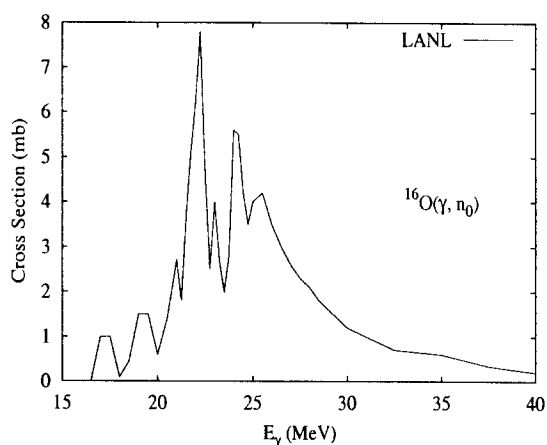
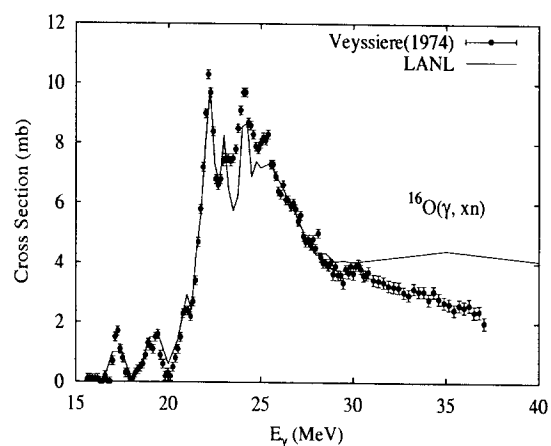
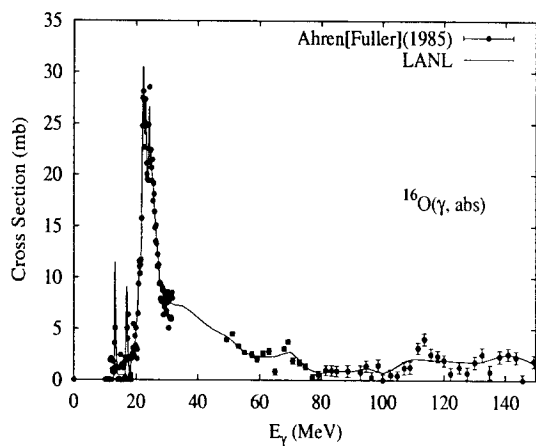


The photoabsorption cross section was evaluated based on the experimental data of Bates [Bat89], up to 35 MeV. Above this energy, the absorption cross section was calculated from the QD model.

The calculated results of the emission channel by the GNASH code are in agreement with the experimental data of Bates [Bat88] for $(\gamma, 1nx)$ reaction cross sections, but are larger than the measurements of Jury [Jur82] for the (γ, xn) and $(\gamma, 2nx)$ reaction cross sections.

$\gamma + {}^{16}\text{O}$

Abundance (%)	Threshold Energies (MeV)								
	γ, n	γ, p	γ, t	$\gamma, \text{He-3}$	γ, α	$\gamma, 2n$	γ, np	$\gamma, 2p$	$\gamma, 3n$
99.76	15.66	12.13	25.03	22.79	7.16	28.89	22.96	22.34	52.06



Our evaluation of photonuclear reactions on oxygen follows, to a large extent, the analysis described by Fuller [Ful85].

The photoabsorption cross section was evaluated based on the data of Ahrens [Ahr75], that extend up to 150 MeV. Below 30 MeV, a constant value of 2.78 mb was subtracted from these data, as recommended by Fuller, in order to make these data consistent with the sum of other (γ, n) , (γ, p) , *etc.* data. However, no such subtraction was made for energies above 50 MeV since this would result in negative cross sections, and a smooth transition was used for the absorption cross section from 30 to 50 MeV.

The Hauser-Feshbach statistical theory cannot be immediately applied in the analysis of photonuclear reactions on oxygen, since there are significant contributions from direct reactions. In particular the (γ, n_0) and (γ, p_0) processes, which result in the residual nucleus being left in its ground state, account for a significant fraction of the photonuclear cross section (particularly for incident energies below 30 MeV). Therefore we first evaluate the (γ, n_0) and (γ, p_0) cross sections from the available experimental data. We adopt Fuller's recommendations for these data. In the case of the p_0 data, these are based on the inverse process of proton capture. These evaluations were extended to 45 MeV based on Phillips' [Phi79] measurements for n_0 and the p_0 results shown in this same paper which are of the same magnitude from 30-45 MeV. Above 45 MeV, because

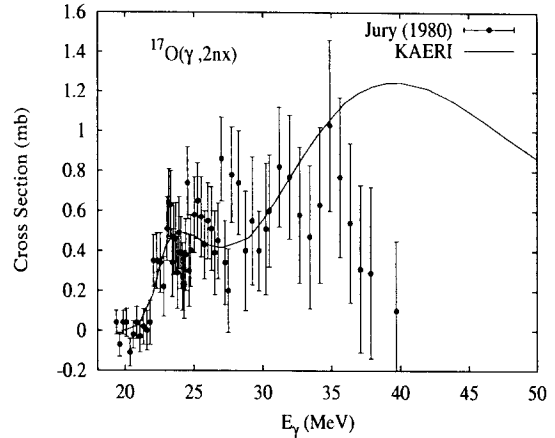
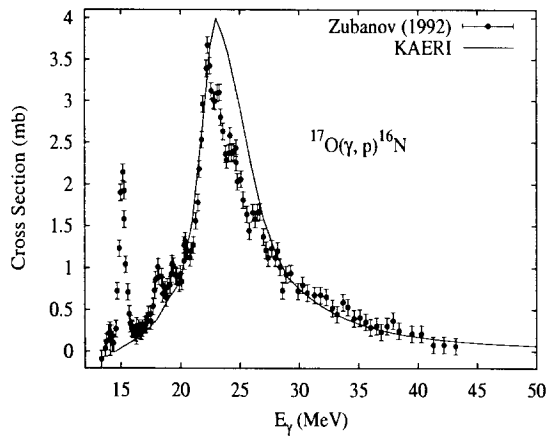
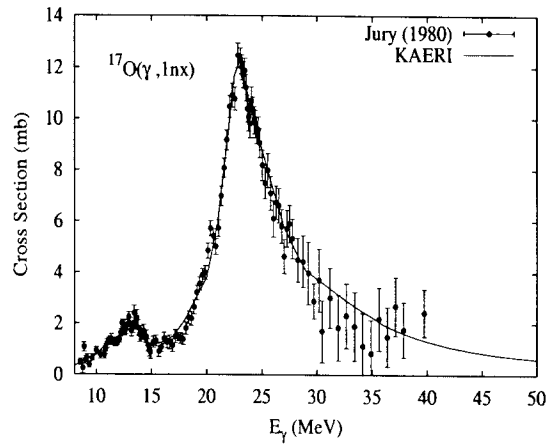
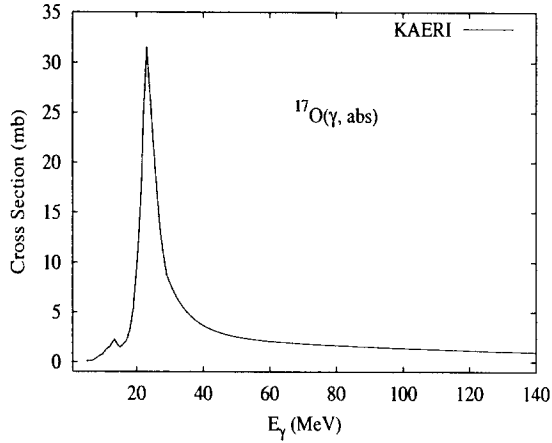
of a lack of other information, we based the n_0, p_0 cross sections on those for carbon [Mat76], since the carbon and oxygen n_0, p_0 data are of similar magnitude to oxygen at 30 MeV.

For the n_0 and p_0 cross sections we provide angular distributions using Legendre polynomials. These were obtained from Phillip's paper [Phi79], for both n_0 and p_0 . (Note that Phillips' text describing the p_0 polynomials is not consistent with the data in his figure 7; Phillips advised us to use the graphical data rather than that based on the text.) Above 40 MeV, these angular distributions were simply extended, unmodified, up to 150 MeV. This is not physically correct [Cha95a], though its impact in transport calculations will be generally small due to the small magnitude of n_0, p_0 cross sections above 40 MeV.

The remaining cross section after (γ, n_0) and (γ, p_0) processes have occurred is modeled with the GNASH code, and represented in the ENDF file using MT5. Preequilibrium and compound decay processes are included. The resulting neutron emission contribution, when added to the (γ, n_0) cross section, was compared with Fuller's evaluation, and other measurements [Vey74, Ber80, Kne75] and good agreement was obtained.

$\gamma + {}^{17}\text{O}$

Abundance (%)	Threshold Energies (MeV)								
	γ, n	γ, p	γ, t	$\gamma, \text{He-3}$	γ, α	$\gamma, 2n$	γ, np	$\gamma, 2p$	$\gamma, 3n$
0.04	4.14	13.78	18.62	18.76	6.36	19.81	16.27	25.26	33.03



The photoabsorption cross section has not been measured. However, there are experimental data for $(\gamma, 1nx)$, (γ, p) , $(\gamma, 2nx)$ and (γ, xn) reaction cross sections by Jury [Jur80]. We relied on the GUNF and GNASH codes to infer the absorption cross section in the GDR regime, so as to model accurately the Jury's measured data. The absorption cross section above the GDR, up to 140 MeV, was taken from QD model calculations.

The calculated results for the emission channels by the GNASH code are in good agreement with the Jury data for $(\gamma, 1nx)$, $(\gamma, 2nx)$ and (γ, xn) reaction cross sections. Overall agreement was also seen for the calculated results for (γ, p) reaction cross sections with the experimental data of Zubanov [Zub92] except the sharp resonance at 15.2 MeV, which is due to the direct capture mechanism.